ISTITUTO NAZIONALE DI FISICA NUCLEARE

Sezione di Padova

INFN/BE-82/2
19 Luglio 1982

U. Fasoli, G. Galeazzi, P. Pavan, D. Toniolo, G. Zago and R. Zannoni: DEFORMATION EFFECT IN THE FAST NEUTRON TOTAL CROSS SECTION OF ALIGNED ^{59}Co

Servizio Documentazione
dei Laboratori Nazionali di Frascati

Istituto Nazionale di Fisica Nucleare
Sezione di Padova

INFN/BE-82/2
19 Luglio 1982

DEFORMATION EFFECT IN THE FAST NEUTRON TOTAL CROSS SECTION OF ALIGNED ^{59}Co

U. Fasoli, P. Pavan, D. Toniolo, G. Zago, R. Zannoni
Istituto di Fisica dell'Università di Padova, and INFN - Sezione di Padova

and

G. Galeazzi
INFN - Laboratori Nazionali di Legnaro

ABSTRACT.

The variation of the total neutron cross section, $\Delta\sigma_{align}$, on ^{59}Co due to nuclear alignment of the target in the beam direction, has been measured over the energy range from 0.8 to 20 MeV, employing a cobalt single-crystal with a 34% nuclear alignment degree. The results show that $\Delta\sigma_{align}$ oscillates from a minimum of - 5% at about 2.5 MeV to a maximum of +1% at about 10 MeV. The data were successfully fitted by optical model coupled-channel calculations. The coupling terms were deduced from a model representing the ^{59}Co nucleus as a vibrational ^{60}Ni core coupled to a proton-hole in a $(1f\,7/2)$ shell, without free parameters. The optical model parameters were determined by fitting the total cross-section independently measured. The theoretical calculations show that, at lower energies, $\Delta\sigma_{align}$ depends appreciably on the coupling with the low-lying levels.

[NUCLEAR REACTIONS $^{59}\vec{Co} + n$, E_n = 0.8 - 20 MeV; measured σ_T and deformation effect $\Delta\sigma_{align}$; data analyzed by coupled-channel calculations; deduced otpical model parameters; no free parameters used in coupling terms.]

1. - INTRODUCTION.

During the last decade a new method for obtaining information about the nuclear shape different from those based on the investigation of effects originated by electric charge nuclear distribution, has been developed. This method consists in observing the variation of the yield of certain nuclear reactions associated to the alignment of the target nuclei bombarded by neutral or charged particles[1].

In principle the alignment is possible for all nuclei having a magnetic moment through the combined action of strong magnetic field and low temperature. But in practice, owing to technical difficulties, this possibility is at present restricted to only a few nuclides.

Among these there are ^{165}Ho and ^{59}Co whose high hyperfine field allows one to obtain an appreciable alignment degree with temperature of some hundred of mK for the first and of few tens of mK for the second.

Particularly convenient as nuclear probes for this purpose, both for physical and instrumental reasons, are the fast neutrons with which the electromagnetic interactions are negligible and are therefore more suitable than charged particle to look the nuclear matter distribution with smaller heating effect which reduce the target alignment.

The first experiment of this kind was performed by Wagner et al.[2]. Marshak et al.[2] by measuring the so called "deformation effect" on fast neutron transmission on a ^{165}Ho aligned target, confirmed the interpretation of the giant resonances on total neutron cross-section given by Peterson[3] and furnished precise value for the ^{165}Ho deformation parameter.

An extension of this experiment to lower energies was later performed at Legnaro[4], where the ^{165}Ho shape was further investigated in a new type of experiment, that is by observing the deformation effect on fast neutron elastic scattering on an aligned ^{165}Ho target[1]. This experiment, although technically much more difficult than a transmission experiment, revealed the potentiality of the new method in obtaining, together with an optical model analysis, precise information about the nuclear shape.

The next nuclide to be investigated was ^{59}Co, whose alignment became possible with the advent of the dilution refrigerators. The first experiment on an aligned ^{59}Co target was performed by Fisher et al.[5] who measured the alignment effect on neutron transmission through a cobalt single-crystal aligned by refrigeration up to about 30 mK, with an alignment degree of 16% at five spot energies between 1 and 2 MeV and at 15. 9 MeV.

Althoug the explored low energy region were rather limited and the presence of large fluctuations in the total cross-section have limited the applicability of the optical model, the results of this experiment were such as to suggest the opportunity of improving the experiment, extending the explored energy range to higher energies, increasing the statistical accuracy and using an higher alignment degree of the target making use of the most recent progresses in cryogenics.

In the experiment here described, preliminary reported in Ref. (6), the deformation effect on ^{59}Co was measured in the neutron energy interval varying continously from 0. 8 to 20 MeV with a greatly improved statistics, on a target having an alignment degree of 34%.

The ^{59}Co is situated in a region where nuclei with collective rotational spectra do not exist, even though electric quadrupole moments, in particular for ^{59}Co, definitely greater than those of single particle, have been measured in atomic spectroscopy experiments[7-9].

Also the shape of the neutron photonuclear cross-section for nuclei in this region[10-12] shows some characteristics that indicate the existence of a permanent deformation. However attempts to explain the experimental data with theoretical previsions based upon rigid deformation, hydrodynamic, vibrational, and dynamic-collective models have not given fully satisfactory results[12].

This seems to indicate that the nuclear structure of ^{59}Co is more complex than that described by these models.

Davies et al.[13] suggested that the nuclear deformation, resulting from measurements of electric quadrupole moment of odd nuclei, in regions where the even-even nuclei exhibit vibrational characteristics, was due to the interaction between the odd nucleon (or hole) and the vibrational core which was partially polarized by the interaction.

Therefore the lowest energy levels of odd cobalt isotopes have been described as originated by the coupling between the nikel vibrational core and a proton-hole[14-18].

Although the results of theoretical calculations based on these models are not entirely satisfactory, they describe rather well some experimental data such as the parameters of the first excited levels as energies, spins, and parities, the spectroscopic factors in direct reactions and the transition probabilities.

These results induced us to attempt to describe n-^{59}Co scattering following the method outlined in Ref. (19), which is essentially an extension of the method introduced by Tamura[20].

2. - THE EXPERIMENT.

2. 1. - Experimental arrangement and electronic apparatus.

The experimental apparatus for the measurement of the neutron transmission variation associated with the alignment of the cobalt target is displayed in Fig. 1.

The cobalt single-crystal C, aligned by means of the ^{3}He-^{4}He dilution refrigerator R, is crossed by the neutron beam generated in the neutron source S, collimated by various collimators and detected by counter D.

The neutron beam was produced by stopping a 4 MeV deuteron beam in a natural lithium target 1 mm thick; the beam was supplied by the 7 MV CN Van de Graaf accelerator at Legnaro, it was pulsed at a frequency of 10^{6} Hz, with pulse-width of 2 ns FWHM.

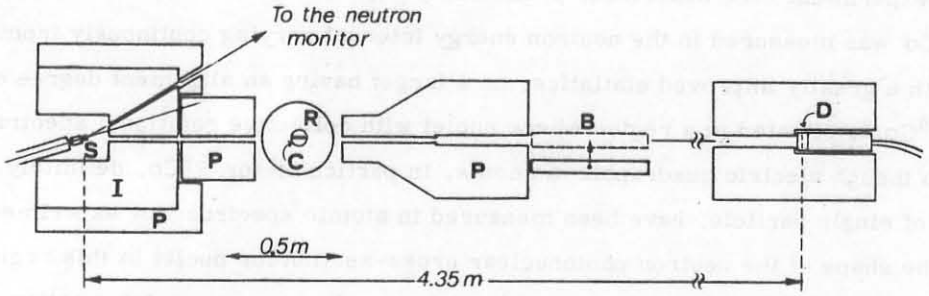

FIG. 1 - Experimental apparatus. S, neutron source; P, paraffin screens; I, iron screens; D, neutron detector NE 213 scintillator with a paraffin and $LiCO_3$ screen; B, iron shadow bar; C, cobalt single-crystal inside the dilution refrigerator R.

The deuteron current, of about 0.5 μA, controlled by a current integrator, was limited by a circular tungsten diaphragm having a 3.5 mm diameter, located very near to the target.

Neutrons were generated on ^{7}Li mainly through the reactions (d,n), (d,n') and (d,n$\alpha\alpha$) having Q-values respectively of 15.03, 12.13 and 15.12 MeV. A small contribution is also due to (d,n) reactions on ^{6}Li present in the target with an isotopic abundance of 7%. Neutrons were also generated by the oxygen present in the lithium target which was partially oxydated, and by the carbon present as contaminant. A time-of-flight spectrum of the source neutrons is represented in Fig. 2 where the contributions of various reactions are indicated.

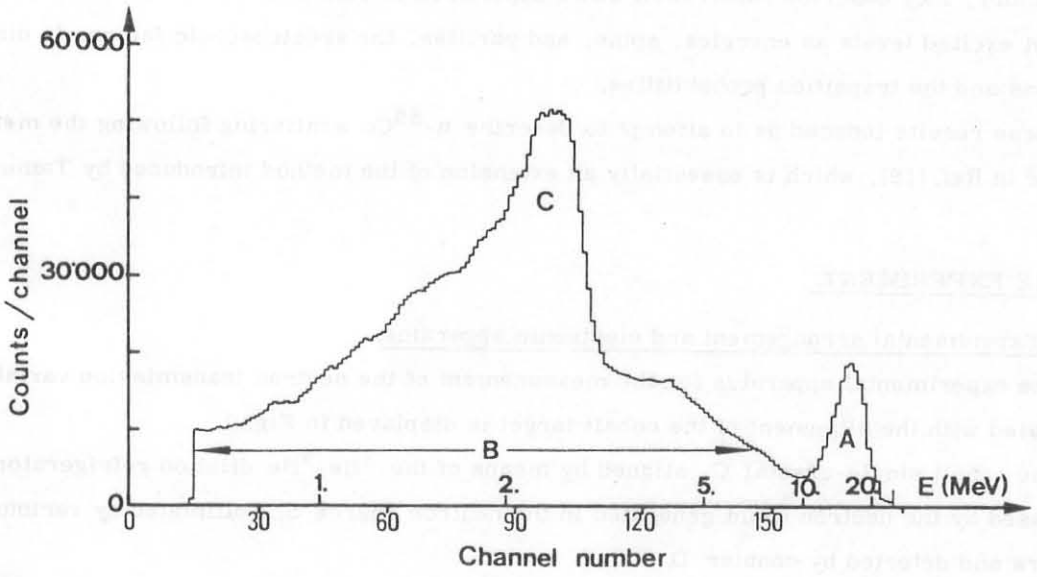

FIG. 2 - Time-of-flight and energy spectrum of the incident neutron beam (background subtracted). A, B and C indicate neutron groups generated respectively: A by the (d,n) and (d,n') reactions on ^{7}Li, B by the (d,n$\alpha\alpha$) reaction on ^{7}Li, and C by (d,n) and (d,n') reactions in carbon and oxygen.

The lithium target yield was very stable both in intensity and spectral shape over several days of deuteron beam bombardament.

The presence of the large masses of the refrigerator and the relatively high intensity and energy of the neutron beam obliged the use of heavy screening of iron and paraffin, in order to reduce the neutron background.

Two channels having a diameter of 1 cm drilled in the iron block surronding the neutron source, at angles of $\pm 12^{o}$ with respect to the incident neutron direction, define two neutron beams which are symmetrical and hence equal in intensity and spectral shape, one impinging into the cobalt sample and detected by the main detector and the second going to the neutron monitor.

The neutron detectors were both formed by a liquid scintillator NE 213 contained in cylindrical glass capsule 2" large and 1" thick, viewed by 56 AVP photomoltipliers, located 4.35 m from the neutron source.

A conventional time-of-flight technique was used, equipped by pulse-shape discrimination, with a neutron detection bias of 0.5 MeV.

The time-of-flight spectra of the two neutron detectors were simultaneously registered through an acquisition system SADIC[21], one line with a HP 2100 computer.

The system presents the same dead-time, less than 2%, for the two counters. The dead--time correction was therefore unnecessary.

The simultaneous registration of the two time-of-flight spectra allowed us to perform the "channel-by-channel monitoring". This consists in referring the countings of the neutrons transmitted in the different time-of-flight intervals and registred in the different time-of--flight channels, to the countings of the corresponding channels of the neutron monitor detector.

In such a way possible systematic errors due to time fluctuations of the shape of the incident neutron spectrum, due, for example, to variations of the oxygen and carbon contamination of the target are drastically reduced.

The energy scale of Fig. 2 has been deduced by the time-of-flight over the flight base of 4.35 m. The time origin was defined by means of the prompt gamma-peak generated by the deuteron pulse impinging on the target and the time scale measured by calibrated cables. A check of the time-energy relation was performed by observing the position of well known resonances in the n-^{12}C total neutron cross-section.

The experimental energy resolution, due mainly to the width of the deuteron pulse of 2 ns, was 1.9% at 1 MeV, 5% at 10 MeV and 7% at 20 MeV.

2. 2. - The refrigerator and the aligned cobalt target.

It is known that in a hexagonal cobalt single-crystal the ^{59}Co nuclei aligne themselves spontaneously in the direction of the c-axis of the crystal at temperatures lower than tens of millikelvin, even in absence of magnetic field[23]. For this reason cobalt single-crystals activated to form ^{60}Co are commonly used as low temperature thermometers since the alignment degree is a well known function of the temperature.

In this experiment the ^{59}Co target was formed by two cobalt single-crystals, grown in this laboratory using the Czochralsky method[24], having the form of truncated cones with a total mass of 45 g. The c-axis directions of the crystals were controlled by optical and X-ray methods[24]. They resulted parallel to the geometrical axes of the cones to within a few degrees. The two crystals were soft-soldered inside a small copper block forming the bottom of the mixing chamber of the refrigerator. In order to insure a good thermal contact, the two cavities in the copper block housing the crystal were machined into the form of conical holes having the same taper angle as the two crystals, which, during the soft soldering operation, were pressed inside the holes.

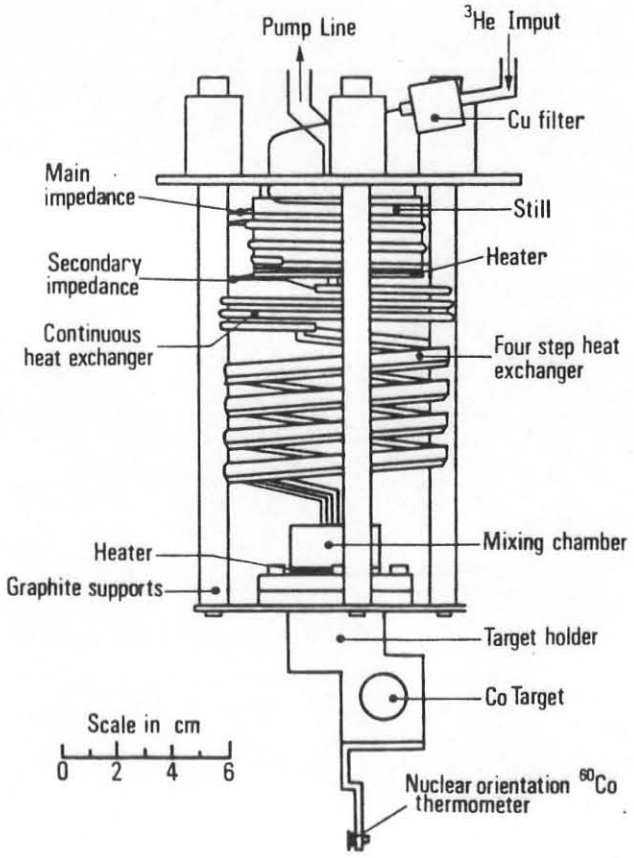

FIG. 3 - Schematic diagram of the dilution refrigerator with the target.

The total thickness of the two crystals was 2.370 cm and the common c-axis was parallel to the neutron beam.

Fig. 3 is a scheme of the refrigerator. The concentrated ^{3}He coming from the condenser is cooled down to the still temperature $\simeq$ 0.7 K and then enters the continuous heat exchanger through a secondary impedance. Four step heat exchangers subsenquently lower the concentrated ^{3}He temperature down to $\simeq$ 18 mK before it enters the mixing chamber. The temperature were typically 60 mK at the exit of the continuous exchanger and 55, 35, 25, 18 mK at the exit of the first, second, third and fourth step heat exchanger respectively.

Particular care was taken in the construction of the step heat exchangers which are of the type de-

scribed by Niinikoski[22].

Four OFHC copper bars with a 0.8 x 1.2 cm rectangular section 10 cm long where choosen. Two circular bores parallel to the length of the bars were drilled, one with a diameter of 0.3 cm for the concentrated stream and another with a diameter of 0.5 cm for the diluted stream. They were partially filled with copper sponge except for an empty bore (0.1 cm diameter) for the concentrated stream and another (0.15 cm in diameter) for the diluted stream. The copper sponges were obtained by filling the bores with copper powder and then syntering it in a furnace at 900 °C for several hours in hydrogen atmosphere.

The lowest temperature obtained in the mixing chamber without Co target was (15.0 ± 1.4) mK with a ^{3}He circulation rate of 50 μmole/sec.

The temperature of the target during the experiment was monitored by means of carbon resistor thermometers calibrated by means of a cerium-magnesium nitrate thermometer and by a ^{60}Co nuclear orientation thermometer[25] soft soldered to the mixing chamber very near to the ^{59}Co target.

The average temperature of the target during the experiment was 18.5 mK, with variations not exceding ± 1 mK.

The nuclear alignment degree of the cobalt single-crystal is calculable, as a function of the temperature by means of the formulae reported, for example, by Lounasmaa[26]. The value of the hyperfine parameter $H\mu/kI$ was considered equal to 1.07×10^{-2} K[27]. At the temperature of (18.5 ± 1) mK one finds $B_2/B_{2\,max} = (0.34 \pm 0.02)$.

2. 3. - Experimental procedure.

We expected the "deformation effect" to be small (of the order of percents). It was therefore important to minimize all the possible causes of spurious effects. To this purpose a careful control of the cobalt target position with respect to the neutron beam was performed. The position of the cobalt target inside the refrigerator was first optically checked at room temperature with the refrigerator tails removed and then at low temperature by means of X-rays. A displacement of the target of about 2 mm was observed. It was due to the thermal contraction of the supporting materials of the cryostat and was in good agreement with the calculations based on known thermal expansion coefficients of the materials.

Secondly, with the refrigerator open, the cobalt target position was controlled optically by a transit located in place of the main neutron detector, oriented in order to observe the center of the neutron source.

Finally the neutron beam profile crossing the cobalt target was determined by moving in small steps horizontally and vertically the whole refrigerator at liquid helium temperature. With such a procedure it was estimated that the cobalt target was centered on the neutron beam axis to within few tenths of a mm. The diameter of the neutron beam at the position of the cobalt target (having a minimum diameter of 10 mm) was fixed to 8 mm by carefully

choosing the diameters of the neutron beam collimators, expecially of that in front of the main neutron detector.

A possible spurious effect due to small lateral fringes of the neutron beam crossing the copper around the cobalt is minimized by the fact that the copper total neutron cross--section is almost equal to that of cobalt.

A second source of spurious effects may be due to time drifts of the electronics. This effect is obviously enhanced if the transmissions through the warm and the cold target are performed at long intervals of time. The time required to cool the target from about 1 K (target unaligned) to the minimum temperature of 18.5 mK reached in this experiment is around 10 hours.

Errors due to this effect have been minimized by adopting the "null method" here described.

The neutron transmission through the single-crystal cobalt target first unaligned and then aligned was compared to the transmission through a second (identical in the nuclear areal density) polycrystalline and therefore unaligned cobalt target, located laterally parallel and very near to the first.

The comparison was made by exposing the two targets alternately to the same neutron beam by moving the whole refrigerator laterally on wheels running on precision rails. The alternating period of a few minutes was sufficiently short to render negligible the temporal drifts of the electronics and of the deuteron beam pulsing apparatus. The alternated exposure of the two targets to the neutron beam was controlled by an integrator of the deuteron beam current. At intervals of the order of an hour the neutron background was measured by intercepting the neutron beam by the iron shadow bar (Fig. 1). The background was of the order of 1-2% for energies lower than 2 MeV and smaller than 1% for energies from 2 to 20 MeV.

The "deformation effect" $\Delta\sigma_{align}$ was measured, with the procedure previously outlined, in a "cold" run, with the target aligned at the temperature of 18.5 mK. The cold run was preceded and followed by "warm" runs respectively at 77 K and 1 K (target with zero alignment) performed in order to check the absence of spurious effects. At the end of the experiment the absolute total neutron cross-section of the cobalt was also measured, using the same procedure and removing the second polycrystalline cobalt target.

The deformation effect $\Delta\sigma_{align}(E_j)$ as a function of the incident neutron energy E_j, was calculated by the formula

$$\Delta\sigma(E_j) = (1/nt)\ln\left[T_2(E_j)/T_1(E_j)\right] \qquad (1)$$

where $n = 0.896 \times 10^{23}$ is the number of the cobalt nuclei per cm^3 in the target, $t = 2.370$ cm its thickness and $T_1(E_j)$ and $T_2(E_j)$ quantities proportional to the neutron transmission

through the aligned cobalt target and the unaligned reference polycrystalline target respectively. That is :

$$T_1(E_j) = \Sigma_i \left[N_{1i}(E_j)/M_i(E_j) \right] \quad \text{and} \quad T_2(E_j) = \Sigma_i \left[N_{2i}(E_j)/M_i(E_j) \right] \qquad (2)$$

where $N_{1i}(E_j)$ and $N_{2i}(E_j)$ are the neutron detector countings relative to the i_{th} alternating cycle, corrected for the background and corresponding to the energy E_j, j being the time-of-flight channel number, and $M_i(E_j)$ the corresponding monitor counts. The whole time-of-flight interval has been divided into 150 equal channels each one about 2 ns wide, 2 ns being the approximate time resolution.

2. 4. - Experimental results.

The results of the measurement are reported in Fig. 4. Fig. 4a represents the sum of the countings of the two warm runs, which were equal within errors. The average relative difference between the transmissions through the unaligned single-crystal and the polycrystalline reference target was $(6 \pm 3) \times 10^{-4}$. The spurious effects were therefore negligible in

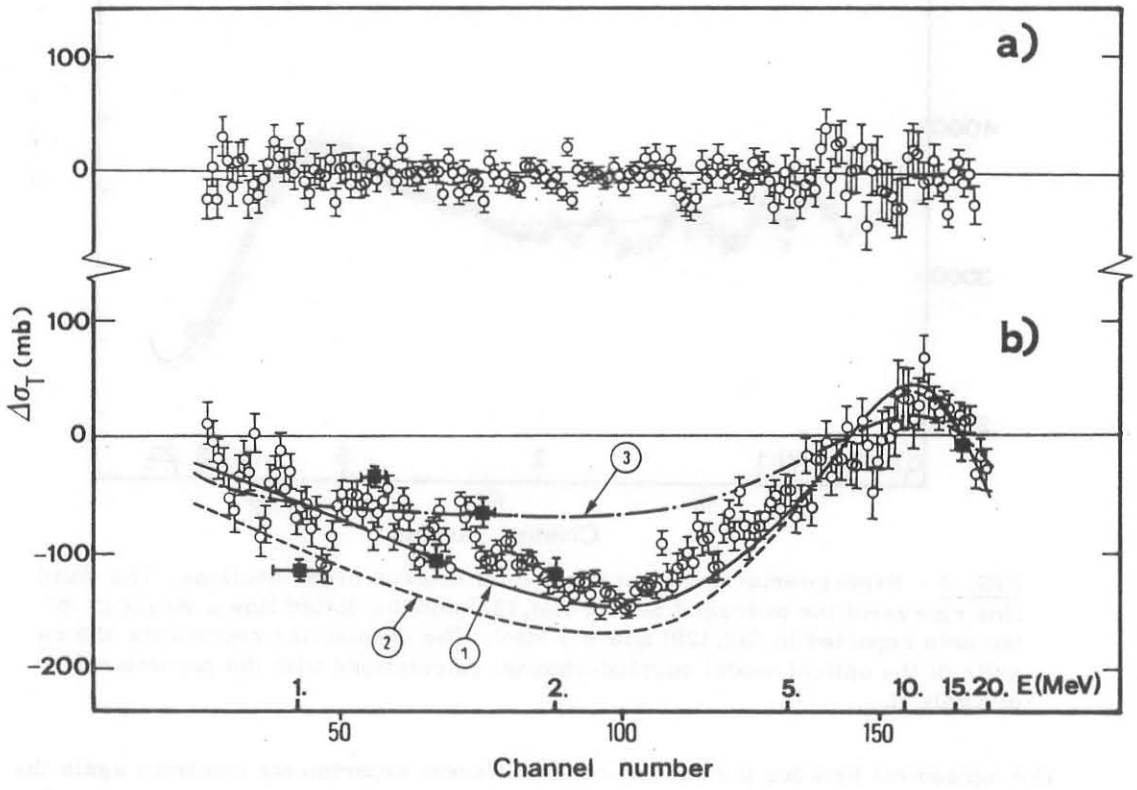

FIG. 4 - a) Difference between the cross sections of the unaligned single-crystal and the polycrystalline reference target. b) Experimental and theoretical deformation effect $\Delta\sigma_{align}$ as a function of the incident neutron energy. The full points are the data of Ref. (5). Curve 1 : $7^-/2$, $9^-/2$, $3^-/2$ coupled levels, $\beta_2 = 0.238$. Curve 2 : only $7^-/2$ level, $\beta_2 = 0.238$. Curve 3 : $7^-/2$, $9^-/2$, $3^-/2$ coupled levels, $\beta_2 = 0.15$.

comparison with the deformation effect, reported in Fig. 4b, which was of the order of some percents.

The errors indicated in Fig. 4 are statistical. They vary as a function of the neutron energy as a consequence of the non-uniform shape of the incident neutron energy spectrum (Fig. 2).

In Fig. 4b the six experimental points obtained by Fisher et al.[5] are also reported, normalized to our results by supposing the effect proportional to the alignment degree (0.34 in the present experiment and 0.16 of Ref. (5)). The agreement is remarkably good.

In Fig. 5 the cobalt total neutron cross section, measured in the present experiment, is reported together with those of other authors. The solid line in the figure has been obtained by properly averaging, over energy intervals corresponding to our energy resolution, the data obtained at Karlsruhe[28] with very high resolution and statistical accuracy (6177 points between 0.36 and 32 MeV and $\Delta t/D = 0.070$ ns/m). The dotted line taken by Ref. (29) represents a visual fit above 3 MeV of data measured by Foster and Glasgow and by Carlson and Barschall.

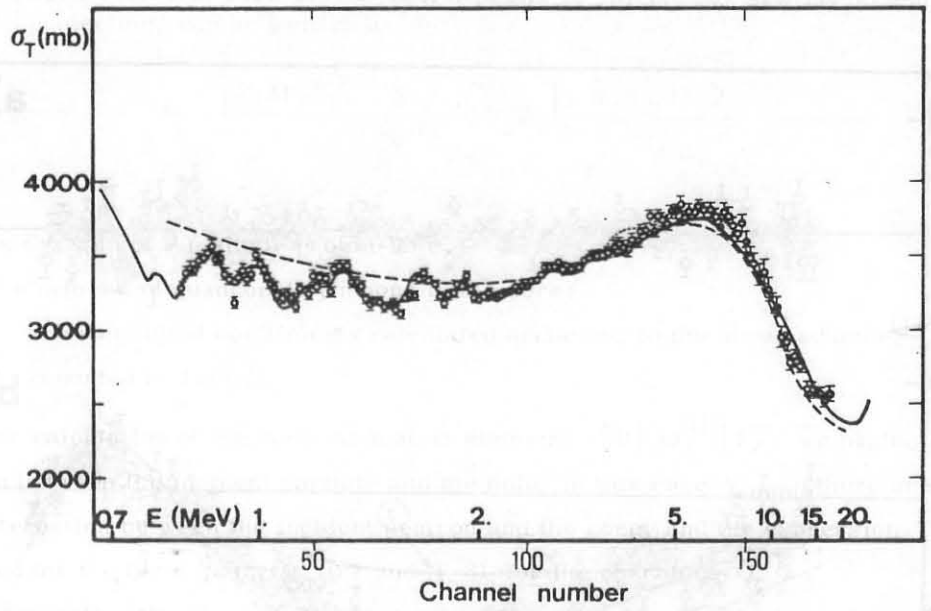

FIG. 5 - Experimental and theoretical total neutron cross sections. The solid line represent the averaged data of Ref. (28) and the dotted line a visual fit of the data reported in Ref. (29) above 3 MeV. The dashed line represents the results of the optical model coupled-channel calculations with the parameters of Table II.

The agreement between the results of the different experiments confirms again the validity of the present experimental procedure.

Particularly good is the agreement between our data and the Karlsruhe data at neutron energies below about 2 MeV where large fluctuations are apparent.

The oscillating trend versus energy of $\Delta\sigma_{align}$ of ^{59}Co recalls a similar shape already observed by Marshak et al.[2] for the deformation effect on ^{165}Ho, which has been clearly explained by a coupled-channel calculation based on the hypothesis that ^{165}Ho is a rigid rotor having a quadrupole deformation parameter $\beta = 0.33$.

3. - THEORETICAL ANALYSIS.

3. 1. - Coupled-channel optical model for ^{59}Co.

In the coupled-channel optical model formalism, the coupling between scattering states is usually described as in Ref. (20) (to the formulas therein containd we shall later refer with the letter T), by the operator T-26

$$V_{coupl} = \sum_{t\lambda} v_\lambda^{(t)}(r)\,(Q_\lambda^{(t)} \cdot Y_\lambda) \qquad (3)$$

where:

- t discriminates terms of different physical characters but of the same tensorial rank λ;
- $v_\lambda^{(t)}$ are form factors deduced from the general form of the optical potential;
- $Q_\lambda^{(t)}$ indicates an operator which operates only on the coordinates of the target nucleus.

The matrix elements of V_{coupl} between scattering states of total angular momentum J, resulting from the coupling of a neutron with orbital momentum ℓ, spin s, total angular momentum j with states of the target nucleus having angular momentum I, represented as $|\ell jI\rangle$, can be deduced using a straightforward calculation and are given by

$$\langle \ell jI | V_{coupl} | \ell' j' I' \rangle = \sum_{t\lambda} v_\lambda^{(t)}(r) \langle I || Q_\lambda^{(t)} || I' \rangle A(\ell jI, \ell' j' I', \lambda Js) \qquad (4)$$

with the geometrical factor A given by T-28.

The physical characteristics of the target nucleus are included in the reduced-matrix elements $\langle I || Q_\lambda^{(t)} || I' \rangle$ which interconnect the lowest excitation states of the target nucleus.

In the case of ^{59}Co a conspicuous number of papers[14, 16, 17, 18, 30] describe the low-lying levels in terms of states of vibrational nucleus ^{60}Ni coupled with single particle (or quasi particle) states of a proton-hole.

Keeping in mind the procedure of Refs. (16) and (30), we have used for ^{59}Co a description of the low-lying states of this nucleus as states of a proton-hole in the configuration $(1f\frac{7}{2})^{-1}$ coupled with a vibrational harmonic core containing up to a maximum of 3 phonons. The characteristic of the vibrational core have been assumed to be those of ^{60}Ni[31]; in particular the quadrupole phonon energy has been assumed to be equal to that of the lowest 2^+ level, namely $\hbar\omega_2 = 1.33$ MeV. In accordance with the data of both Refs. (31) and (32)

β_2 = 0. 238 has been assumed as the value of the deformation.

The coupling constant $\langle 1f\frac{7}{2}\left|r\frac{dV}{dr}\right|1f\frac{7}{2}\rangle$ has been deduced from the wave-function calculated with a Saxon-Woods potential including a spin-orbit term[33] and with Coulomb term due to a uniform spherical charge distribution[30].

Such a description reproduces only approximately the ground-state electric quadrupole moment (q_{th} = 0. 61 eb, q_{exp} = 0. 41 ± 0. 03 eb)[34], the sequence of the experimental levels, their energies and the transition rates $B(E_2)$. It is however to be pointed out that this description does not contain free parameters.

A better reproduction of the experimental data has been obtained by Stewart et al.[15] introducing quasi-hole states coupled with a vibrational anharmonic quadrupole core. The particle-vibration coupling intensity, however, has been calculated with a best fit on the experimental data.

In the present description a generic low-lying state of ^{59}Co, characterized by a set of quantum numbers (n, I, M), n being the order number of the level, I and M the spin and relative 3rd projection, can be written as

$$|nIM\rangle = \sum_{jN_2R_2} a^{nI}_{jN_2R_2} \left| j, N_2R_2; IM \right\rangle \qquad (5)$$

where:

j is the spin of the single proton-hole;

R_2 the number of quadrupole phonons in the core;

$a^{nI}_{jN_2R_2}$ are numerical coefficients calculated according to the above scheme[16, 30] and reported in Table I.

In the calculation of the reduced-matrix elements $\langle I' \left|\left| Q^{(t)}_\lambda \right|\right| I \rangle$, we neglected the interaction between the incident particle and the hole. In this case V_{coupl} therefore reduces to the interaction between the incident neutron and the core, and the expression T-13 may be applied for the form factors $v^{(t)}_\lambda(r)$ and T-31 for the operators $Q^{(t)}_\lambda$.

Consequently, the single proton-hole plays the role of core polarizer element, without giving any contribution to the coupling between scattering states; its contribution to the diagonal part of the scattering is incorporated in the optical potential, whose parameter determination will be described later.

Since, according to this view, Q_λ operates on the collective (vibrational) coordinates of the core only, the application of the Wigner-Eckart's theorem for composite systems (see e. g. eq. (1A-72), pag. 84 of Ref. (35)) leads to

TABLE I - Numerical values of the coefficients $a^{nI}_{\frac{7}{2}^- N_2 R_2}$ for ^{59}Co. The level energies are in MeV.

N_2 R_2	n	1	2	3	4	5	6
	I	$\frac{7}{2}^-$	$\frac{3}{2}^-$	$\frac{9}{2}^-$	$\frac{11}{2}^-$	$\frac{5}{2}^-$	$\frac{7}{2}^-$
0 0		0.6160	0.0	0.0	0.0	0.0	0.6341
1 2		0.6440	0.6739	0.6613	-0.6561	-0.5840	-0.1040
2 0		0.2412	0.0	0.0	0.0	0.0	-0.4149
2 2		-0.2115	0.6140	-0.3792	-0.2665	-0.4516	0.3923
2 4		0.2669	0.2382	0.5474	-0.6081	-0.5079	-0.2269
3 0		-0.0524	0.0	0.0	0.0	0.0	0.1587
3 2		0.1514	0.1590	0.1680	-0.1530	-0.0963	-0.3775
3 3		0.0055	-0.2615	-0.0566	-0.1485	0.3638	-0.0820
3 4		-0.0559	0.1359	-0.2266	0.0649	-0.2155	0.1610
3 6		0.0536	0.0	0.1910	-0.2812	-0.0821	-0.0744
E_{exp}		0.0	1.10	1.19	1.46	1.48	1.74
E_{theor}		0.0	1.23	0.93	1.28	2.15	2.85

$$\langle n' I' \| Q_\lambda \| nI \rangle = \sum_{j N_2 R_2} \sum_{j' N_2' R_2'} a^{nI}_{j N_2 R_2} a^{n'I'}_{j' N_2' R_2'} \cdot \tag{6}$$

$$\cdot \hat{I}\hat{I}' (-1)^{j+R_2+I'+2} \begin{Bmatrix} j & R_2 & I \\ \lambda & I' & R_2' \end{Bmatrix} \langle N_2' R_2' \| Q_\lambda \| N_2 R_2 \rangle ;$$

the reduced-matrix elements of the second member are given by the expressions T-36, T-37, T-39 and for 3-phonon states by the formula (6B-42) of Ref. (36), pag. 690.

3. 2. - Optical-model parameter determination.

The potential describing the n-^{59}Co interaction in optical model coupled-channel formalism is written as

$$V(r, \theta, \phi) = -(V+iW) \frac{1}{1+\exp((r-R)/a)} - 4iW_D \frac{\exp((r-\bar{R})/\bar{a})}{(1+\exp((r-\bar{R})/\bar{a}))^2} - \tag{7}$$

$$- V_{so} (\sigma \cdot \ell) \hbar_\pi \frac{1}{ar} \frac{\exp((r-R)/a)}{(1+\exp((r-R)/a))^2}$$

R and $\overline{R}$ are expressed by

$$R = R_o\left(1 + \Sigma \alpha_{\lambda\mu} Y_{\lambda\mu}(\theta,\phi)\right) \qquad \overline{R} = \overline{R}_o\left(1 + \Sigma \alpha_{\lambda\mu} Y_{\lambda\mu}(\theta,\phi)\right)$$

with $R_o = r_o A^{1/3}$, $\overline{R}_o = \overline{r}_o A^{1/3}$, A being the mass number of the target nucleus.

The parameters to be calculated with a best-fit procedure on the experimental data are V, W, W_D, V_{so}, r_o, $\overline{r}_o$, a, $\overline{a}$.

The values of the optical model parameters have been determined starting from the set used by Fisher[37] in a spherical optical model calculation. With these parameters he fitted the data of total neutron cross-section in the interval 0.5 - 16 MeV and the data of the angular n-^{59}Co elastic scattering at 1, 4 and 14 MeV.

We kept the parameters V_{so} and W fixed and equal to those of Fisher (7 and 0 MeV respectively) while the others, including α and β, the coefficients of energy dependence of V and W_D, have been calculated with a best-fit on the total experimental cross section in the interval 0.8 - 20 MeV as reported in Refs. (38) and (39). The result of the fit is displayed in Fig. 5.

At neutron energies below 10 MeV the experimental σ_T presents large fluctuations, as can be seen in the original data of the high energy resolution measurement of Ref. (28). Therefore we have averaged the original data with an energy resolution equal to that of our experiment, and these averaged data are reported in Fig. 5.

Even with this energy resolution the fluctuations of σ_T are still very pronunced and in the best-fit procedure we have assumed a suitable mean calculated with a still smaller resolution.

The coupled-channel optical model calculations require very long computer times; moreover the non linearity of the least-squares problem and the high number of parameters to be determined make the problem very difficult. The discrepancies between the experimental and theoretical cross sections are mainly ascribable to difficulties of this kind.

The number of coupled levels is also an important factor in computer time consumption. All our calculations have been performed by coupling together the first three levels ($\frac{7}{2}^-$ ground state and the first $\frac{3}{2}^-$ and $\frac{9}{2}^-$ excited states).

Finally it should be noted that all calculations have been performed with complex form-factors (T-13) and the number of partial waves considered in the interaction was determined by the condition that the penetrability coefficients relative to the neglected waves should be smaller than 10^{-5}.

The optical model parameters so obtained are reported in Table II.

The elastic scattered neutron angular distribution, calculated with the parameter values of Table II and reported in Fig. 6, have also been compared with the experimental data at 1.0[37], 4.0[37], 7.05[38], 9.0[39], 11.0[40] and 14.0[37] MeV. The agreement is good at the

energies 1, 4, 7.05 and 14 MeV, and reasonable, though less satisfactory, at 9 and 11 MeV.

TABLE II - Optical model parameters values obtained from the best-fit; it should be noted that $V = V_o + \alpha E$, $W_D = W_o + \beta E$, E being the neutron energy in MeV.

V_o (MeV)	α	W (MeV)	W_o (MeV)	β	V_{so} (MeV)	r_o (fm)	a (fm)	$\bar{r}_o$ (fm)	$\bar{a}$ (fm)
49.72	-0.5349	0.0	14.23	0.0068	7.0	1.262	0.6078	1.414	0.222

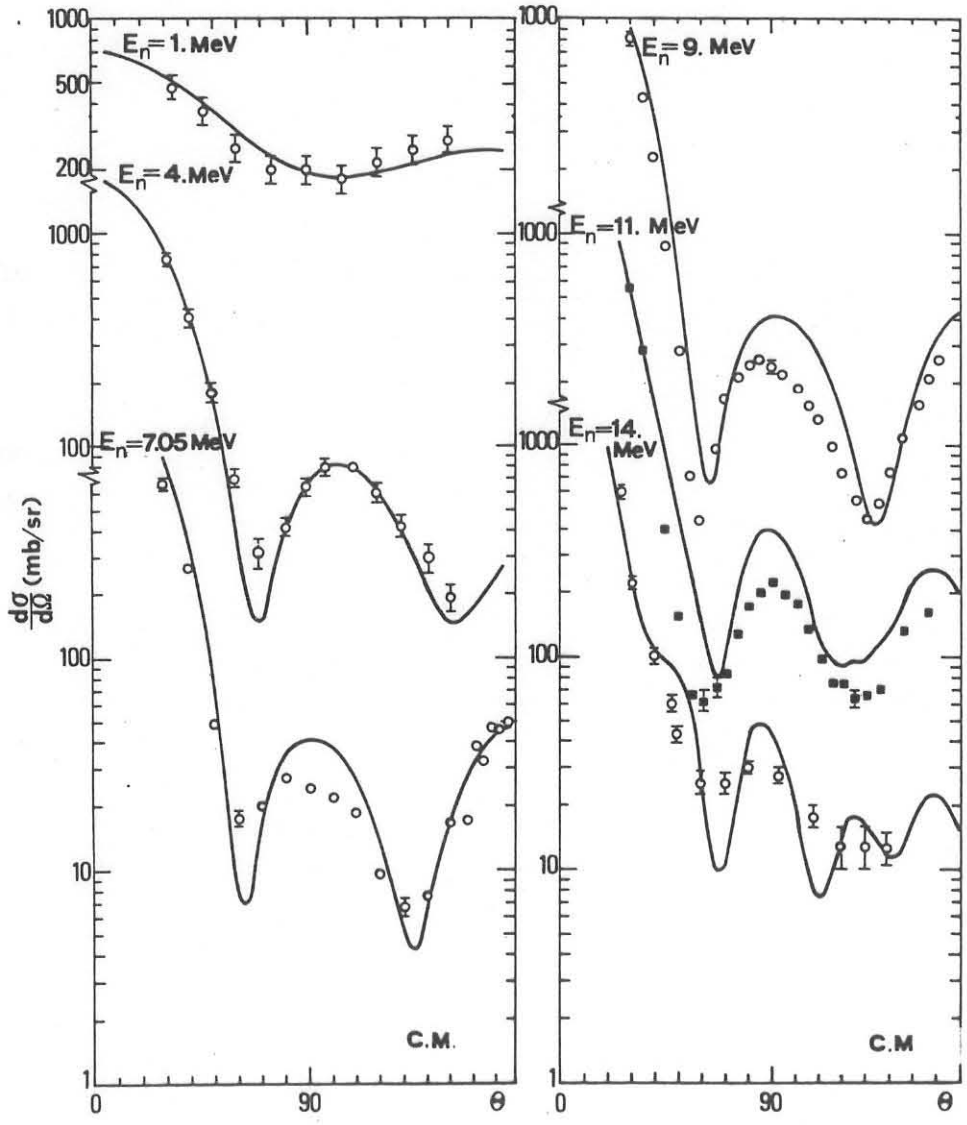

FIG. 6 - Experimental and theoretical angular distributions for elastic scattered neutrons at 1.0[37], 4.0[37], 7.05[38], 9.0[39], 11.0[40] and 14.0[37] MeV. A compound-elastic scattering contribution was added at 1 MeV as in Ref. (37) and a constant contribution of 10 mb/sr was added at 4 MeV.

3. 3. - Deformation-effect calculation.

In order to calculate the deformation effect, it is necessary to know the parameters describing the nuclear target orientation degree given by the populations P_M, relative to different magnetic substrates M, at 18.5 mK, temperature at which the experiment was performed. The values of P_M calculated from the temperature and the hyperfine coupling strength[5] are reported in Table III.

TABLE III - Magnetic substate populations P_M in the beam direction, in the ^{59}Co aligned target, at the temperature of 18.5 mK.

M	$-\frac{7}{2}$	$-\frac{5}{2}$	$-\frac{3}{2}$	$-\frac{1}{2}$	$\frac{1}{2}$	$\frac{3}{2}$	$\frac{5}{2}$	$\frac{7}{2}$
P_M	0.226	0.131	0.082	0.061	0.061	0.082	0.131	0.226

The deformation effect was consequently calculated as the difference between the total cross sections of an aligned and an unaligned target.

The results of the calculations, reported in Fig. 4b, curve 1, relative to $\beta_2 = 0.238$ as previously said, agree very well with the experimental data.

We have attempted to estimate the importance of the level coupling in the calculation of $\Delta\sigma_{align}$. It is apparent from the curve 2 of Fig. 4b that the ground state alone does not completely account for the shape of $\Delta\sigma_{align}$, especially at neutron energies lower than 4 MeV.

The introduction of at least the first excited state is decisive in order to obtain a good agreement with the experimental data, while the introduction of other excited level does not appreciably improve this agreement.

On the contrary, the introduction of one or more energy levels does not substantially change the total cross section σ_T.

In Fig. 7 is represented the dependence of $\Delta\sigma_{align}$ on β_2, the deformation parameter of the vibrational core, for five values of the incident neutron energy, while the curve 3 of Fig. 4b represents the dependence of $\Delta\sigma_{align}$ on the incident neutron energy for $\beta_2 = 0.15$.

Both figures indicate that the dependence of $\Delta\sigma_{align}$ on β_2 is very critical.

By a best fit procedure, based on the curves of Fig. 7, one obtains $\beta_2 = 0.224$. This value is not substantially different from 0.238, which is relative to curve 1 of Fig. 4b, and yet within the range of the values of β_2 obtained by other experiments.

4. - CONCLUSIONS.

The deformation effect in the fast neutron transmission through an aligned ^{59}Co target, having a nuclear alignment degree $B_2/B_{2max} = 0.34$, was measured in the neutron energy

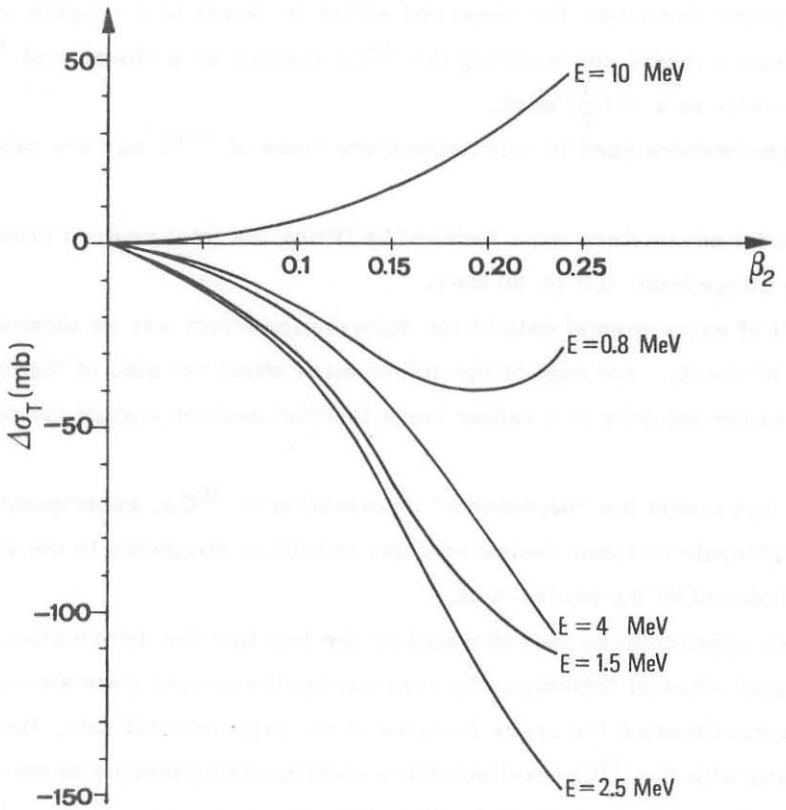

FIG. 7 - The deformation effect $\Delta\sigma_{align}$ as a function of β_2, for five values of the incident neutron energy.

interval from 0.8 to 20 MeV.

About 150 points were taken evenly-spaced at intervals of 2 ns, which is the time-of--flight experimental resolution. Spurious effects of different nature were controlled to be negligible.

The observed deformation effect oscillates smoothly versus neutron energy from a value of - 5% of the total cross-section around 2.5 MeV to + 1% at 10 MeV and then decreases below - 1% at 20 MeV. Below 1.5 MeV large fluctuations are apparent similar in position and shape to those present in the total cross-section curve, independently measured.

The six energy points measured by Fisher et al.[5] are in good agreement with the present results.

The oscillatory character of the effect recalls a similar feature of the deformation effect on ^{165}Ho observed by Marshak et al.[2] and clearly explained by an optical model calculation as due to the rigid prolate deformation of ^{165}Ho.

This is not the case of ^{59}Co which belongs to a nuclear mass region where rotational spectra characteristic of large rigid nuclear deformation, are not present, while odd nuclei show appreciably large ground state electric quadrupole moment.

We have therefore described the observed effect in terms of a coupled channel calculation starting from a model representing the ^{59}Co nucleus as a vibrational ^{60}Ni core coupled to a proton-hole in a $(1f\frac{7}{2})$ shell.

The coupling parameters used in calculations are those of ^{60}Ni and are taken from the literature.

The optical model parameters were deduced by fitting the total neutron cross-section in the neutron energy range from 0.8 to 20 MeV.

A very good fit of experimental data of the deformation effect was so obtained.

The goodness of the fit, not only of the deformation effect but also of the total and differential scattering cross-sections in a rather large incident neutron energy range, validates the model.

In the light of this model the "permanent" deformation of ^{59}Co, experimentally evidenced by electric quadrupole moment measurements, should be attributed to the vibrational core polarization induced by the proton-hole.

This conclusion appears to be corroborated by the fact that the deformation effect, calculated by the coupled-channel formalism by considering the ground state alone, already represents in first approximation the gross features of the experimental data. However, the fact that the coupling with the ^{59}Co excited states contributes noticeably to the deformation effect evidences the importance of observing the effect at energies larger than few MeV in order to extract a reliable value of the ground state electric quadrupole moment.

ACKNOWLEDGEMENTS.

We wish to thank L. Badan and G. Bressanini for the continuous invaluable co-operation during the construction of the cryogenic and electronic apparatus and during the performance of the experiment.

Thanks are also due to the Staff of the National Laboratory of Legnaro and in particular to R. Preciso and L. Donà of the Mechanical Workshop where the dilution refrigerator was constructed.

Finally we acknowledge the kind co-operation of C. Rossi Alvarez in the use of the data acquisition system SADIC, and Mrs. M. Evans Prosperi who revised the English text.

REFERENCES.

(1) - U. Fasoli, G. Galeazzi, D. Toniolo, G. Zago and R. Zannoni, Nuclear Phys. A284, 282 (1977), and the bibliography therein indicated.

(2) - R. Wagner, P. D. Miller, T. Tamura and H. Marshak, Phys. Rev. 139, 29 (1965); H. Marshak, A. Langsford, T. Tamura and C. Y. Wong, Phys. Rev. C2, 1862 (1970).

(3) - J. M. Peterson, Phys. Rev. 125, 955 (1962).

(4) - U. Fasoli, G. Galeazzi, D. Toniolo and G. Zago, Lett. Nuovo Cimento 6, 485 (1973).

(5) - T. R. Fisher, A. R. Poletti and B. A. Watson, Phys. Rev. C8, 1837 (1973).

(6) - U. Fasoli, G. Galeazzi, P. Pavan, D. Toniolo, G. Zago and R. Zannoni, Lett. Nuovo Cimento 27, 207 (1980).

(7) - D. von Ehrenstein, Ann. d. Phys. 7, 342 (1961).

(8) - W. J. Childs and L. S. Goodman, Phys. Rev. 170, 50 (1968).

(9) - K. Murakawa, J. Phys. Soc. Jpn. 27, 1690 (1969).

(10) - S.C. Fultz, R. L. Bramblett, J. T. Caldwell, N. E. Hansen and C. P. Jupiter, Phys. Rev. 128, 2345 (1962).

(11) - G. Baciu, G. C. Bonazzola, B. Minetti, C. Molino, L. Pasqualini and G. Piragino, Nuclear Phys. 67, 178 (1965).

(12) - R. A. Alvarez, B. L. Berman, D. D. Faul, F. H. Lewis Jr. and P. Meyer, Phys. Rev. C20, 128 (1979).

(13) - K. T. R. Davies, G. R. Satchler, R. M. Drisko and R. H. Bassel, Nuclear Phys. 44, 607 (1963).

(14) - L. Satpathy and S. C. Gujrathi, Nuclear Phys. A110, 400 (1968).

(15) - A. Covello and V. R. Manfredi, Phys. Letters 34B, 584 (1971).

(16) - M. Montagna, Thesis, University of Padua (1971) (unpublished).

(17) - K. W. Stewart, B. Castel and B. P. Singh, Phys. Rev. C4, 2131 (1971).

(18) - J. M. G. Gomez, Phys. Rev. C6, 149 (1972).

(19) - J. L. C. Ford Jr., C. Y. Wong, T. Tamura, R. L. Robinson and P. H. Stelson, Phys. Rev. 158, 1194 (1967).

(20) - T. Tamura, Rev. Mod. Phys. 37, 679 (1965).

(21) - A. Buscemi, M. De Poli, C. Rossi-Alvarez and R. Zanon, in 'Proceedings of the 1st European HP-1000 User Conference', Amsterdam, 1981.

(22) - T. O. Niinikosky, Nuclear Instr. and Meth. 97, 95 (1971).

(23) - M. A. Grace, C. E. Johnson, N. Kurti, R. G. Scurlock and R. T. Taylor, Phyl. Mag. 4, 948 (1959).

(24) - U. Fasoli and P. Pavan, Report INFN/TC-80/1 (1980).

(25) - Supplied by Oxford Instriments Co., Oxford, England.

(26) - O. V. Lounasmaa, 'Experimental Principles and Methods below 1 K' (Academic Press, 1974).

(27) - D. A. Shirley, in 'Hyperfine Structure and Nuclear Radiation', ed. by E. Matthias and D. A. Shirley (North-Holland, 1968), pag. 985.

(28) - S. Cierjacks, P. Forti, D. Kopsch, L. Kropp, J. Nebe and H. Unseld, KFK Report 1000, Suppl. 2 (1969).

(29) - M. D. Goldberg, S. F. Mughabghab, B. A.Magurno and V. M. May, Brookhaven National Laboratory Report BNL 325 (1966).

(30) - A. Covello and V. R. Manfredi, Boll. Soc. Ital. Fisica 79, 90 (1970).

(31) - R. L. Auble, Nucl. Data Sh. 28, 103 (1979).

(32) - G. Bruge, J. C. Faivre, H. Faraggi and A. Bussiere, Nuclear Phys. A146, 597 (1970).

(33) - K. Bleuler, M. Beiner and R. de Tourreil, Nuovo Cimento 52B, 45 (1967).

(34) - H. J. Kim, Nucl. Data Sh. 17, 485 (1976).

(35) - A. Bohr and B. R. Mottelson, 'Nuclear Structure' (Benjamin, 1969), Vol. 1.

(36) - A. Bohr and B. R. Mottelson, 'Nuclear Structure' (Benjamin, 1975), Vol. 2.

(37) - T. R. Fisher, H. A. Grench, D. C. Healey, J. S. McCarthy, D. Parks and R. Witney, Nuclear Phys. A179, 241 (1973).

(38) - E. Ramström and P. A. Göransson, Nuclear Phys. A284, 461 (1977).

(39) - D. E. Velkley, D. W. Glasgow, J. D. Brandenberger, M. T. McEllistrem, J. C. Manthuruthil and G. P. Poirier, Phys. Rev. C9, 2181 (1974).

(40) - J. C. Ferrer, J. D. Carlson and J. Rapaport, Nuclear Phys. A275, 325 (1977).